Forced Wetting and Hydrodynamic Assist

Terence D. Blake,* Juan-Carlos Fernandez-Toledano, and Joël De Coninck

Laboratory of Surface and Interfacial Physics, University of Mons, 7000 Mons, Belgium

* E-mail: terrydblake@btinternet.com

Introduction

It is well known that air entrainment sets the ultimate limit to coating speeds. It is also known that air entrainment can be postponed to higher line speeds by manipulating coating flows to generate what has been termed 'hydrodynamic assist' [1]. There is increasing evidence that the benefit is associated with geometric or hydrodynamic confinement of the moving contact line [1-3]. In addition, experiments have shown that the conditions that allow higher line speeds in curtain coating also reduce the apparent dynamic contact angle, suggesting a direct link [4,5]. However, the mechanism by which the flow might affect wetting speeds and the dynamic angle has not been established – although several theories have been advanced. Here we develop an earlier suggestion [6] that an intense shear stress in the vicinity of the moving contact line can assist surface tension forces in compensating for contact-line friction. This reduces the velocity-dependence of the contact angle and so postpones air entrainment. Hydrodynamic assist is then a natural consequence of forced wetting that emerges when the contact line is driven by a very strong and highly confined flow.

Approach

We use large-scale molecular dynamics (MD) simulations to compare forced, steady wetting with our previous results for spontaneous spreading of liquid drops. We focus on two aspects: the velocity dependence of the dynamic contact angle and the details of the fluid flow, especially that near the moving contact line. The advantage of MD over experiment is that it models bulk behavior in a realistic manner while giving access to the molecular details of the interfaces. Anther strength is that it allows solid-liquid interactions can be adjusted at will.

For the forced wetting simulations we model a liquid bridge between two solid plates moving at an equal speed in opposite directions (Fig. 1). The plate separation H is either 8.85 or 36.1 nm in the z direction. Periodic boundary conditions are enforced in the x and y directions. The numerical methods, base parameters and potentials used are described in our previous publications [7,8]. Further details relating to forced wetting are given in a more recent paper [9]. To summarize, we model the liquids, the solids and their interactions using Lennard-Jones potentials. The liquid phase is composed of 8-atom molecular chains held together by a confining potential.
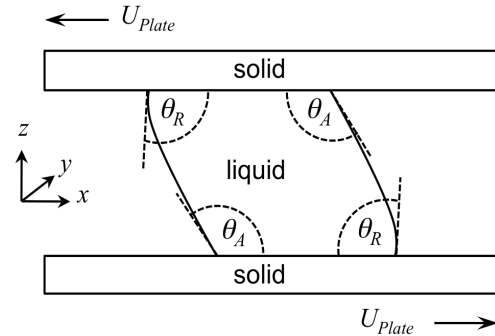

Fig. 1. Forced wetting system.

This increases viscosity and minimizes evaporation. The solid is rectangular square-planar lattice having three atomic layers and bound by a strong harmonic potential. The solid-liquid interactions are adjusted to give a range of equilibrium contact angles from 75° to 135°. Previous work has shown that this yields realistic behavior that accurately replicates real physical systems. Contact angles are measured by fitting a smooth curve (usually a circular arc) to the bulk interface and extrapolating to the solid surface, as in an experiment. Flow velocities are determined by first dividing the liquid into a large number of rectangular cells. We find the positions of the atoms within each cell and then measure the distance and direction that each atom moves over a number of time steps within the simulation. Averaging over a large number of time

steps enables us to retrieve reliable values of all the parameters. Standard methods are used to determine the liquid density $\rho_L = 18.3$ atom/nm^3, viscosity $\eta_L = 0.248$ mPa.s, and surface tension $\gamma_{LV} = 2.49$ mN/m.

Dynamic contact angles and slip

Fig. 2 shows typical results for forced wetting plotted as the surface tension driving force for wetting $f_{CL} = \gamma_{LV}(\cos\theta^0 - \cos\theta_D)$ versus the contact-line velocity $U_{CL} = -U_{Plate}$, where θ^0 and θ_D are, respectively, the equilibrium and dynamic contact angles. To analyze the results and explain our findings we use the molecular-kinetic theory of dynamic wetting (MKT) [6]. This predicts that for a low surface tension liquid:

$$U_{CL} = \gamma_L \left(\cos\theta^0 - \cos\theta_D \right) \big/ \zeta, \tag{1}$$

where ζ is the contact-line friction (in units of shear viscosity). As can be seen the data reveal essentially linear behavior. The resulting values of the contact line frictions are displayed in Fig. 3.
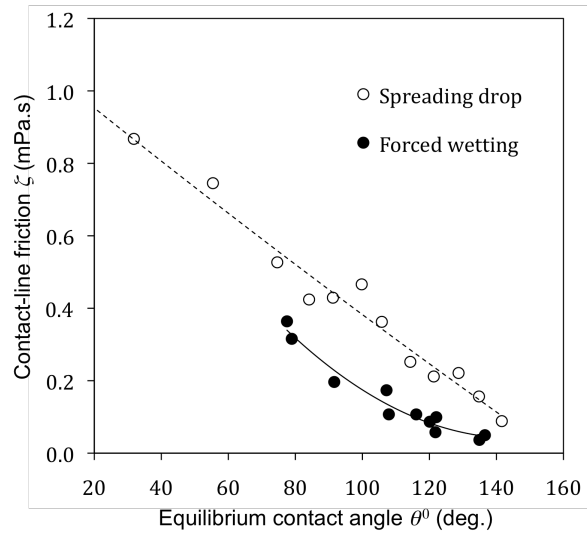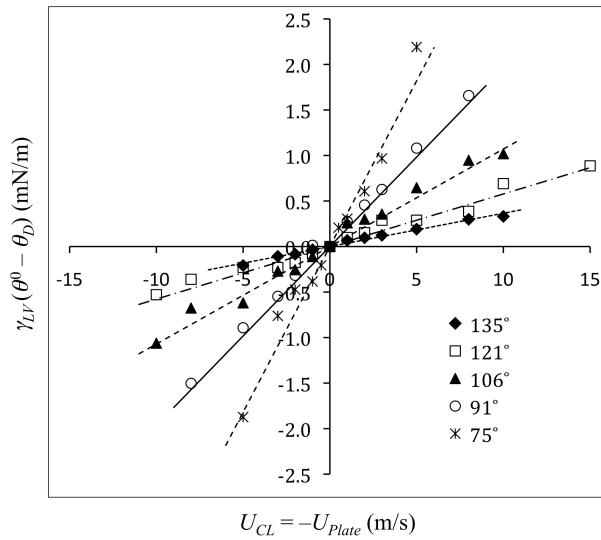

Fig. 2 Surface tension driving force v. contact-line velocity   Fig. 3. Contact-line friction for spreading drops and forced wetting

It is immediately clear that the contact-line frictions for forced wetting are significantly smaller than those found for spreading drops. The reduced friction means that for a given contact-line speed the dynamic contact angles are also different. Advancing contact angles are smaller and receding angles bigger. This is a key result and entirely independent of any theoretical model of dynamic wetting. Our previous spreading drop simulations [7,8] showed that the local, microscopic contact angle is dependent on contact-line velocity and is not simply equal to its equilibrium value, as often assumed. The new data for forced wetting confirm this, but also show that the angle is dependent the nature of the flow. Thus, the reduction in the dynamic contact angles seen in curtain coating under conditions of hydrodynamic assist [4,5] may at least be partly due to a real reduction in the microscopic contact angle, and not just to some change in the degree of viscous bending of the liquid surface at a scale below that of experimental observation (~10 μm). So, what might cause such an effect?

The simulations show that the flow near the solid surface during drop spreading is quite different to that in forced wetting: Figs. 4 and 5, respectively. In the drops, flow is mostly downward towards the solid surface. Flow tangential to the solid is negligible except near the advancing contact line. In contrast,

during forced wetting, the moving plates drive a strong flow at their surfaces. This is as expected, but close inspection reveals that the speed of the flow is significantly less than the speed of the plates U_{Plate}. In other words, there is slip between the liquid and the solid.
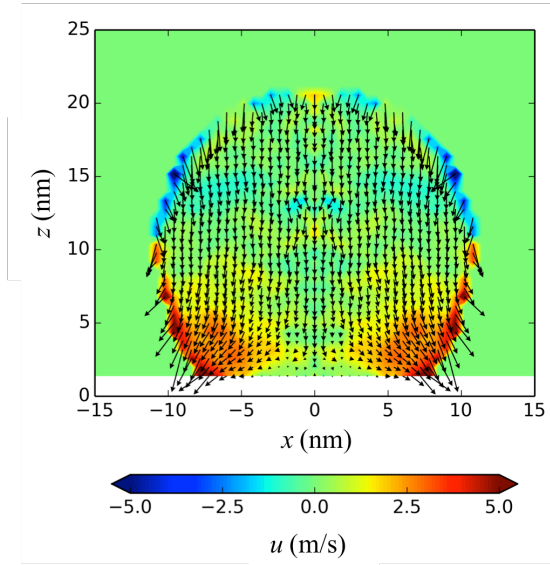

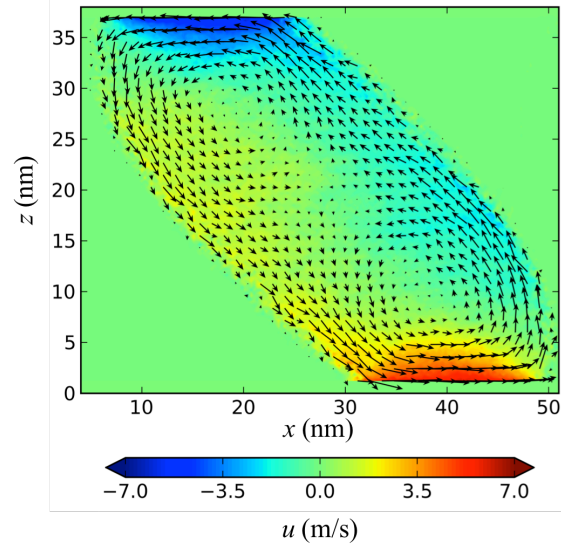Fig. 4. Radial flow inside a spreading drop. Fig. 5. Rotational flow during forced wetting.

Fig. 5 also shows a continuous 'tank-tread' flow around the boundary of the liquid bridge driven by the shear. The shear is present along all the boundaries and at the contact lines. The shear stress generated by the rotational flow is $\eta_L(du_x/dz)$. It is this that is responsible for the slip velocity $U_{Slip} = U_{Plate} - u_{x1}$ against the frictional drag of the solid. Here u_{x1} is the velocity of the first layer of liquid in contact with the solid. If we adopt the linear slip condition proposed by Navier, we can write $\eta_L(du_x/dz) = \beta U_{Slip}$, where $\beta = \eta_L/l_{Slip}$ is the slip coefficient and l_{Slip} is the slip length, *i.e.* the distance into the solid at which the linearly extrapolated fluid velocity vanishes.

At the molecular level, the contact line is a three-phase zone (TPZ) of small but finite thickness δ that approximates that of the confluent solid-liquid and liquid-vapor interfaces. Hence, the shear stress developed across this region by the surface tension driving force is f_{CL}/δ per unit length of the contact line. Our analysis of the drop spreading simulations has shown that the dynamics of molecules within the TPZ is the same as at the general solid-liquid interface. Compared with their comparative freedom in the bulk liquid, the molecules in both surface regions are equally retarded by their interaction with the potential energy landscape of the solid surface. The coefficients of contact-line friction and slip must, therefore, be closely related: specifically, $\beta = \zeta/\delta$. Hence, the shear stress generated by the rotational flow $\eta_L(du_x/dz)$ is equal to $\zeta U_{Slip}/\delta$. Since this operates everywhere along the solid-liquid boundary, *including* the TPZ, the total force driving the contact line will be $f_{CL} = \zeta U_{Slip} + \gamma_{LV}(\cos\theta^0 - \cos\theta_D)$ and Eq. (1) becomes

$$U_{CL} = U_{Slip} + \gamma_L\left(\cos\theta^0 - \cos\theta_D\right). \qquad (2)$$

This should be valid over at least the range of velocities for which there is a linear relationship between f_{CL} and U_{CL}. In consequence, if U_{CL} is significant, the change in the dynamic contact angle required to maintain a given contact-line velocity will be reduced both at advancing and at receding contact lines, with a consequent reduction in the apparent contact-line friction $\zeta = -d(\cos\theta_D)/dU_{CL}$, as observed.

Another way of viewing this is to consider that the contact-line velocity is effectively reduced by the slip velocity to $U_{CL} - U_{Slip} = -u_{x1}$. This provides an immediate connection to hydrodynamic assist, since higher coating speeds are required before θ_D approaches 180° or any other critical angle sufficient to trigger air entrainment. The theoretical model becomes slightly more complicated for real liquids with higher surface tensions than that in our simulations, when the full non-linear MKT equation is required [6,7], although the arguments remain essentially the same [9].

In order to assess how significant the effect of slip is likely to be, it is illuminating to determine the dependence of the dynamic contact angle on the shear stress developed by the flow, or, more simply, its dependence on the shear rate. We have already seen that the shear stress is given by $\eta_L(du_x/dz)$ and that this is equal to $\zeta U_{Slip}/\delta$. It follows that $U_{Slip} = \delta\eta_L(du_x/dz)/\zeta$. Therefore, in order to calculate the change in dynamic contact angle with shear rate using Eq. (2), it remains only to determine δ – all other parameters being known. An estimate of the thickness of the TPZ has been obtained by measuring the z-component of the velocity of the first layer of liquid molecules across the zone as new solid-liquid interface is created or destroyed [9]. This shows a distinct peak, the width of which gives a value of $\delta = 3.52$ nm, which is slightly thicker than the liquid-vapor interface (2.52 nm).

Figure 6 (below) shows the result of evaluating Eq. (2) in the form:

$$\theta_D = \cos^{-1}\left[\cos\theta^0 - \left(\zeta U_{CL}/\gamma\right) + \left(\eta\delta/\gamma\right)\left(du_x/dz\right)\right]. \tag{3}$$

Here, the dynamic advancing contact angle is plotted as a function of shear rate for a range of fixed contact-line velocities from 1 to 10 m/s (capillary numbers Ca = $\eta U_{CL}/\gamma$ from 0.1 to 1). The curves shown are for a system with a solid-liquid interaction that gives an equilibrium contact angle of 91°. If there were no dependence on shear rate, each line would run horizontally across the chart. This is clearly not the case. While the dynamic contact angle does remain essentially constant at low shear rates, once this exceeds a threshold of about 10^8 s^{-1} the angle begins to fall rapidly towards zero. The velocity gradients in our simulations of forced wetting were in the range 10^8 – 10^{10} s^{-1}. Evidently, at sufficiently high shear rates, the value of the advancing contact angle is determined entirely by the flow and can fall well below its equilibrium value.
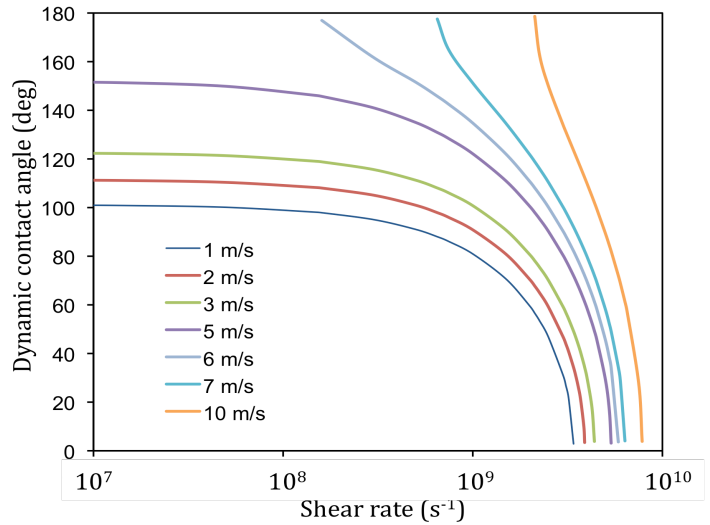

Fig. 6. Variation of the dynamic contact angle with shear-rate at fixed contact-line velocities during forced wetting for an equilibrium contact angle of 91°.

We can estimate of the shear rate at which the flow becomes dominant by comparing the shear stress developed across the TPZ by the surface tension driving force with that generated by the flow. The former is of order γ/δ, i.e. 7×10^5. The latter exceeds this at shear rates $>3\times10^9$. Beyond this point, contact-line friction becomes increasingly unimportant. This remarkable result offers an explanation for the experimental observation that during curtain coating with large curtain heights and very viscous liquids, air entrainment can apparently be postponed to indefinitely high speeds, provided the contact line is confined exactly beneath the falling curtain where the shear rates are greatest [2]. The viscosity/surface tension ratio at which this behavior has been observed are about than 2 orders of

magnitude greater than that in our simulations, so the shear rates can be correspondingly smaller: about 10^7, assuming the thickness of the TPZ is similar, *i.e.* a few nanometers.

In summary, we believe our new work provides a deep insight into the dynamics of wetting and the way in which the local microscopic angle may depend on the nature of the flow and, therefore, on the conditions under in which it is measured. While other factors, such as changes to the degree of interfacial viscous bending and the elimination of displaced air may also play their part, our findings provide a salient explanation for hydrodynamic assist.

References

[1] T. D. Blake, A. Clarke, and K. J. Ruschak, 'Hydrodynamic assist of dynamic wetting,' *AIChE J.* **40** (1994) 229–242.

[2] T. D. Blake, R. A. Dobson, and K. J. Ruschak, 'Wetting at high capillary numbers,' *J. Colloid Interface Sci.* **279** (2004), 198–204.

[3] E. Vandre, M. S. Carvalho, and S. Kumar, 'Delaying the onset of dynamic wetting failure through meniscus confinement,' *J. Fluid Mech*. **707** (2012) 496–520.

[4] T. D. Blake, M. Bracke, and Y. D. Shikhmurzaev, 'Experimental evidence of nonlocal hydrodynamic influence on the dynamic contact angle,' *Phys. Fluids* **11** (1999) 1995–2007.

[5] A. Clarke and E. Stattersfield, 'Direct evidence supporting non-local hydrodynamic influence on the dynamic contact angle,' *Phys. Fluids* **18** (2006, 48109 (2006).

[6] T. D. Blake, 'Dynamic contact angles and wetting kinetics,' in *Wettability*, J. C. Berg, Ed. (Dekker, New York, 1993) pp 251–309.

[7] E. Bertrand, T. D. Blake, and J. De Coninck, 'Influence of solid-liquid interactions on dynamic wetting: a molecular dynamics study,' *J. Phys. Condens. Matter* **21** (2009) 46124.

[8] J. De Coninck and T. D. Blake, 'Wetting and molecular-dynamics simulations of simple liquids,' *Annu. Rev. Mater. Res*. **38** (2008) 1–22.

[9] T. D. Blake, J-C. Fernandez-Toledano, G. Doyen, and J. De Coninck, 'Forced wetting and hydrodynamic assist,' *Phys. Fluids*, **27** (2015) 112101.